Appl. Phys. A 83, 103–106 (2006)
DOI: 10.1007/s00339-005-3463-2

Applied Physics A
Materials Science & Processing

T. HEEG[1,✉]
J. SCHUBERT[1]
C. BUCHAL[1]
E. CICERRELLA[2]
J.L. FREEOUF[2]
W. TIAN[3]
Y. JIA[3]
D.G. SCHLOM[3]

Growth and properties of epitaxial rare-earth scandate thin films

[1] Institut für Schichten und Grenzflächen ISG1-IT and Center of Nanoelectronic Systems for Information Technology (cni), Forschungszentrum Jülich GmbH, 52425 Jülich, Germany
[2] Department of Physics, Portland State University, Portland, Oregon 97207-0751, USA
[3] Department of Materials Science and Engineering, The Pennsylvania State University, University Park, Pennsylvania 16802-5005, USA

Received: 4 September 2005/Accepted: 8 November 2005
Published online: 13 January 2006 •

ABSTRACT Epitaxial rare-earth scandate thin films of 100–1500 nm in thickness have been prepared by pulsed laser deposition on $SrTiO_3$(100) and MgO(100) substrates. Stoichiometry and crystallinity were investigated by Rutherford backscattering spectrometry/channelling (RBS/C), transmission electron microscopy, and X-ray diffraction. Electrical measurements on microstructured capacitors with a $SrRuO_3$ bottom electrode and Au top contacts reveal dielectric constants of 20 to 27, leakage currents of 0.85 to 6 $\mu A/cm^2$ at 250 kV/cm, and breakdown fields of 0.6 to 1.2 MV/cm. The optical bandgaps of the films range from 5.5 to 6 eV. The results substantiate the high potential of rare-earth scandates as alternative gate oxides.

PACS 73.61.Ng; 73.40.Rw; 77.22.Ch; 77.55.+f; 78.40.Ha

1 Introduction

The international technology roadmap for semiconductors (ITRS) emphasises the need for alternative gate dielectrics for silicon-based metal-oxide-semiconductor field-effect transistor (MOSFET) devices [1]. Accordingly, new high dielectric constant (κ) gate dielectrics have gained considerable attention. High-κ dielectrics are expected to provide comparable performance to SiO_2, while simultaneously permitting a thicker dielectric layer to dramatically reduce charge tunnelling through the oxide. Consequently for any alternative dielectric a high κ and a wide bandgap to limit current leakage are of primary importance.

The rare-earth scandates ($REScO_3$, RE denoting a rare earth element) in amorphous or epitaxial form have been proposed as candidates for the replacement of SiO_2 [2]. Their structure is orthorhombic at room temperature, isostructural with $GdFeO_3$ (and $NdGaO_3$, $SrRuO_3$, etc.). For example, the lattice parameters of $GdScO_3$ are $a = 548.8$ pm, $b = 574.6$ pm, and $c = 793.4$ pm; the space group is *Pbnm* [3, 4]. These lattice parameters are favourable for epitaxial growth on silicon. Furthermore, all rare-earth scandates except $EuScO_3$ [5] are predicted to be thermodynamically stable in contact with silicon [2]. Since there is no data available for $LaScO_3$ single crystals, possibly due to its high melting temperature (2290 °C, [4]), the properties reported in this work on epitaxial films are of particular value. Furthermore, initial results on thin amorphous scandate films also indicate properties advantageous for application [6, 7].

✉ Fax: +49-2461-61-4673, E-mail: t.heeg@fz-juelich.de

2 Sample preparation

Epitaxial and amorphous films of $LaScO_3$, $GdScO_3$, and $DyScO_3$ were grown by pulsed laser deposition (PLD), using a KrF excimer laser (wavelength 248 nm, pulse width 20 ns and a fluence of 2.5 J/cm^2). Targets were made by mixing 99.99% pure La_2O_3, Gd_2O_3, Dy_2O_3, and Sc_2O_3 powders, ball milling in isopropanol for 24 h, calcining at 1300 °C for 24 h, pressing into 25 mm diameter targets, and finally sintering at 1500 °C for 12 h. Thin films were deposited in four different PLD chambers utilizing on-axis or off-axis geometries [8–11].

In the on-axis geometry, the substrate is located in the center of the PLD plasma plume. This permits a high deposition rate with a limited area of uniformity (in this case 1×1 cm^2). The substrates are positioned directly onto a SiC resistive heater. An oxygen gas partial pressure of 2×10^{-1} Pa is maintained during the deposition process.

In the off-axis geometry, the substrate surface is oriented parallel to the expansion direction of the plume. This leads to a lower deposition rate, but allows much larger substrates (e.g., up to 2 inch diameter) to be coated uniformly. Radiation heating is provided to both sides of the substrate. Both oxygen and nitrogen gas are used as the process gas at a partial pressure of 1.2×10^{-1} Pa. Nitrogen is admitted in order to investigate the growth of scandates in a non-oxidizing atmosphere [12]. In all setups used, the prepared thin films showed comparable properties. Although the PLD process tends to generate small particulates in the films (droplets or larger particles removed from the target surface), this imposes no restriction because a sufficient area of the sample is unaffected.

Different sets of films were fabricated. $LaScO_3$, $GdScO_3$, and $DyScO_3$ films were deposited in an on-axis geometry on $SrTiO_3$(100) substrates at temperatures from 500 °C to 900 °C to establish the crystalline quality as a function of growth temperature. For optical characterization, epitaxial and amorphous $LaScO_3$, $GdScO_3$, and $DyScO_3$ films were

grown in on-axis geometry on MgO(100) substrates ($1 \times 1\,\mathrm{cm}^2$) with a 10 nm thick $BaTiO_3$ interlayer (necessary for epitaxial growth on MgO) also grown with PLD. For the epitaxial $LaScO_3$ and $GdScO_3$ samples on MgO, a substrate temperature of 750 °C was used, and for the epitaxial $DyScO_3$ 850 °C was used during deposition.

For electrical characterization, films were deposited in on-axis and off-axis geometry onto an epitaxial $SrRuO_3$ quasi-metallic bottom electrode on $SrTiO_3$(100) substrates of $1 \times 1\,\mathrm{cm}^2$ size. The $SrRuO_3$ electrode was also grown by PLD at a temperature of 600 °C in a 15 Pa oxygen ambient. The substrate temperature during scandate film growth was around 1000 °C in off-axis PLD and around 850 °C in on-axis PLD. Finally, circular Au metal top electrodes were deposited by thermal evaporation through a shadow mask to form an array of parallel plate capacitors, with areas ranging from 0.00625 to $0.8\,\mathrm{mm}^2$.

3 Film characterization

Rutherford backscattering spectrometry/channelling (RBS/C) utilizing He^+ ions with an energy of 1.4 MeV was used to investigate the composition and crystalline quality of the films. The computer software RUMP provided the numerical analysis of the RBS data [13]. Figure 1 shows the RBS/C spectra of a 350 nm thick epitaxial $LaScO_3$ film grown on $SrTiO_3$ at 900 °C. The channelling minimum yield $\chi_{\min}$ is 2%, revealing good crystallinity. RBS analysis of a 1.5 μm thick $GdScO_3$ film on a $BaTiO_3$-buffered MgO substrate shows a Gd/Sc ratio of 1.0/1.07 and $\chi_{\min} = 4\%$, indicating that the films are stoichiometric within experimental error and have good epitaxial quality. Similar results were obtained on $BaTiO_3$-buffered MgO substrates for 1.5 μm thick $LaScO_3$ (La/Sc ratio: 1.0/0.97, $\chi_{\min} = 3\%$) and $DyScO_3$ (Dy/Sc: 1.0/0.95, $\chi_{\min} = 4.5\%$).

The RBS/C spectra of $GdScO_3$ deposited onto $SrRuO_3$/$SrTiO_3$ in the on-axis setup show a minimum yield $\chi_{\min} = 6.2\%$, demonstrating epitaxial growth. A better minimum yield of $\chi_{\min} = 3.1\%$ was achieved for $LaScO_3$ on the same electrode/substrate system. For comparison, a 160 nm thick $GdScO_3$ film on $SrRuO_3/SrTiO_3$ deposited in the off-axis setup exhibits an excellent Gd/Sc ratio of 1.0/1.0 as well. The use of nitrogen as a non-oxidizing process gas was tested successfully, because no indication of nitrogen was found in the films by RBS. Similar results were obtained for $LaScO_3$ and $DyScO_3$ films.

The lattice parameters of the films and their orientation were characterized by X-ray diffraction (XRD). An example is shown in Fig. 2 for $LaScO_3$ grown at different substrate temperatures. At 500 °C, only the XRD reflections from the $SrTiO_3$ substrate are detected, whereas at higher growth temperatures (600 °C and up), the XRD peaks from the scandate layer appear.

Four-circle XRD and TEM (described below) indicate that the scandate films crystallized with orthorhombic structure as found in bulk material [3, 4]. The rocking curve full width at half maximum (FWHM) of the $LaScO_3$ 220-reflection of the 900 °C sample is $\Delta\omega \approx 0.1°$, also indicating good crystallinity. The lattice parameters of this film were determined to be $a, b = 584$ pm, $c = 806$ pm using a Nelson–Riley plot [14]. Similar results were obtained for $DyScO_3$ (the epitaxial growth starts at 900 °C, lattice parameters $a, b = 567$ pm and $GdScO_3$ films (epitaxial growth at > 700 °C, lattice parameters $a, b = 570$ pm, $c = 788$ pm). In φ-scans performed on all scandate thin films with (110) orientation using the 226 reflection we observe four peaks separated by 90° indicating that the film is epitaxial and consists of two orientation variants related by a 90° in-plane rotation.

This is also corroborated by transmission electron microscopy (TEM) measurements. Specimens were prepared by conventional cross-sectional TEM techniques, including mechanical grinding, polishing, and dimpling, followed by final Ar-ion milling in a Gatan precision ion polishing system at 4.2 kV to electron transparency. HRTEM studies were carried out using a JEOL 4000EX operated at 400 kV, which has

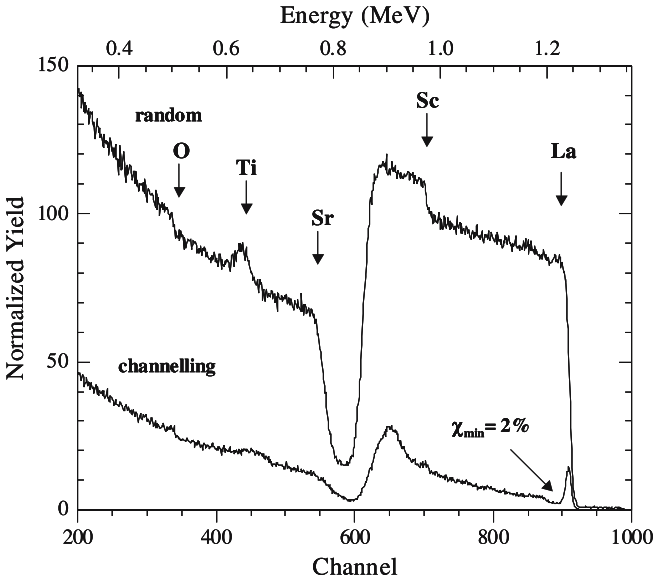

FIGURE 1 RBS random and channelling spectrum of a 350 nm thick $LaScO_3$ film grown epitaxially on $SrTiO_3$ at a substrate temperature of 900 °C. The incident energy is 1.4 MeV, the scattering angle is 170°

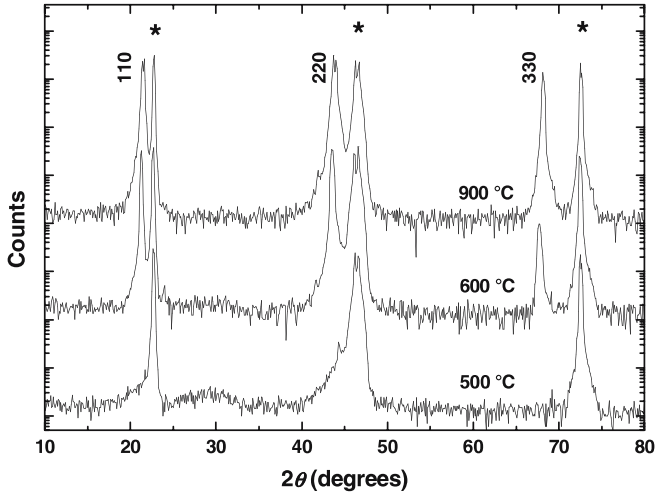

FIGURE 2 XRD θ–2θ-scan of $LaScO_3$ on $SrTiO_3$(100) grown at different substrate temperatures. Substrate peaks are marked with an *asterisk* (∗). The film grown at 900 °C (whose RBS spectra are shown in Fig. 1) has lattice constants $a, b = 584$ pm and $c = 806$ pm, and a rocking curve FWHM of the 220 peak of 0.1°

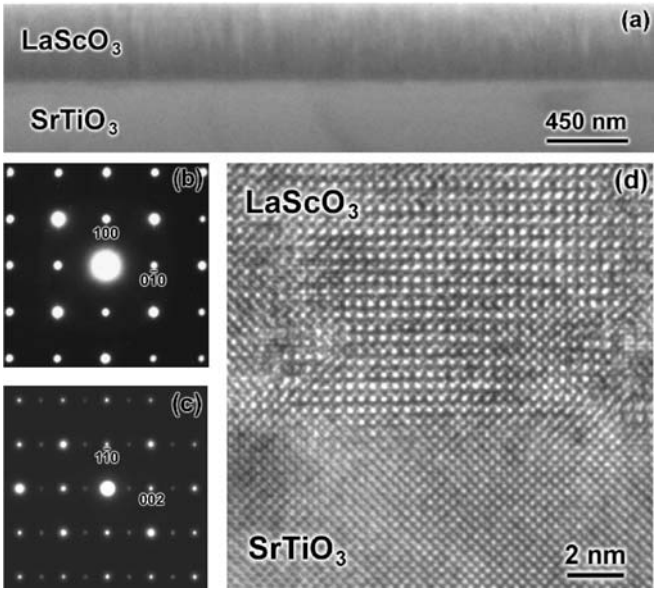

FIGURE 3 TEM characterization of the same $LaScO_3$ film grown on $SrTiO_3$(100) at 900 °C whose RBS spectra are shown in Fig. 1. (**a**) Low magnification image, (**b**) [001] zone axis SAED pattern of the $SrTiO_3$ substrate, (**c**) [110] zone axis SAED pattern of the $LaScO_3$ film, (**d**) HRTEM image of the substrate/film interface

a point-to-point resolution of 0.17 nm. Figure 3 displays the TEM results of the same $LaScO_3$ film whose RBS and XRD spectra are shown in Figs. 1 and 2. Figure 3a is a low magnification cross-sectional TEM image showing a very smooth surface of the film. Figure 3b and c are selected area electron diffraction (SAED) patterns taken from the substrate and the film with the incident electron beam along the same direction, respectively. They are identified as the [001] zone axis diffraction pattern of $SrTiO_3$ and the [110] zone axis diffraction pattern of $LaScO_3$, respectively. The epitaxial growth of the film is evident, and the epitaxial orientation relationship is $(1\bar{1}0)$ $LaScO_3 \parallel (100)$ $SrTiO_3$ with two in-plane variants: [110] $LaScO_3 \parallel$ [001] $SrTiO_3$ and [001] $LaScO_3 \parallel$ [001] $SrTiO_3$ (SAED pattern not shown). A high-resolution transmission electron microscopy (HRTEM) image of the film/substrate interface with the electron beam incident along the [001] zone axis of $SrTiO_3$ is shown in Fig. 3d. One can see that the interface is well defined and no noticeable interdiffusion occurs, despite the high growth temperature (900 °C).

An XRD $\theta - 2\theta$-scan of a $LaScO_3$ film grown on $BaTiO_3$/MgO showed the lattice parameters $a, b = 578$ pm using a Nelson–Riley [14] plot of the $hh0$ peaks. The reference data of bulk $LaScO_3$ are $a = 568$ pm, $b = 579$ pm [3, 4]. The rocking curve FWHM of the 330 reflection is $\Delta\omega \approx 0.43°$. For the $GdScO_3$ and $DyScO_3$ films grown on $BaTiO_3$/MgO, the lattice parameters were determined to be $a, b = 566$ pm and $a, b = 563$ pm, respectively. The bulk data of $GdScO_3$ are $a = 549$ pm, $b = 575$ pm and of $DyScO_3$ are $a = 544$ pm, $b = 571$ pm [3, 4].

4 Optical properties

Absorption measurements [15] on the scandate films on the $BaTiO_3$-buffered MgO revealed an optical bandgap > 5 eV. The amorphous $LaScO_3$ film shows an onset of transmission at 5.5 eV, the epitaxial film at > 5.8 eV. Similar values were obtained for $GdScO_3$ and $DyScO_3$. The results are described in detail elsewhere [16]. They are comparable to photoconductivity measurements, performed on similar samples [7]. The observed bandgap is encouraging for the use as an alternative gate oxide [1, 2].

5 Electrical properties

The impedance of metal–insulator–metal parallel-plate capacitors was measured with an HP4192A impedance analyzer. The results for an epitaxial 105 nm thick $DyScO_3$ film (grown by on-axis PLD) are shown in Fig. 4. In the voltage range from −4 to 4 V, a 0.05 mm^2 electrode capacitor shows a capacitance of about 90 pF almost independent of frequency from 10 kHz to 1 MHz, corresponding to a dielectric constant κ of 21 to 22. The observed losses are low: $\tan\delta$ is in the range from 0.02 (at 10 kHz) to 0.06 (at 1 MHz). Similar results were achieved for $LaScO_3$ ($\kappa = 24 - 27$, $\tan\delta = 0.004 - 0.03$) and $GdScO_3$ ($\kappa = 20$, $\tan\delta = 0.004 - 0.03$). These values correspond well to the results measured on sin-

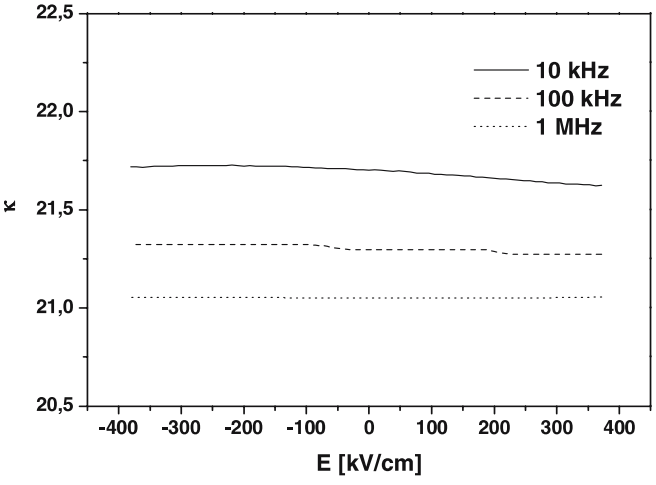

FIGURE 4 Dielectric constant of an epitaxial, 105 nm thick $DyScO_3$ film with $SrRuO_3$ bottom electrode and Au top electrode grown on a $SrTiO_3$(100) substrate at 850 °C

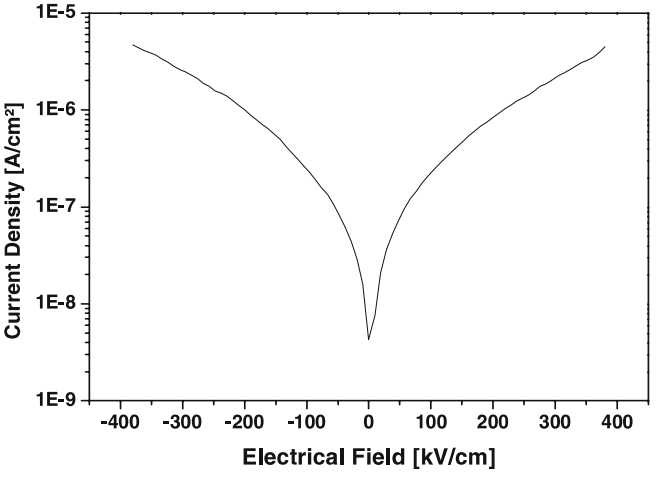

FIGURE 5 Leakage current density of the same epitaxial $DyScO_3$ film whose κ is shown in Fig. 4

gle crystals of $GdScO_3$ and $DyScO_3$ for (110) plates [17]. Comparable results were also observed for samples grown in a nitrogen atmosphere by off-axis PLD.

The leakage currents of the samples were investigated with an HP4155B semiconductor parameter analyzer. A representative result is shown in Fig. 5 for the 0.05 mm^2, 105 nm thick $DyScO_3$ capacitor. Leakage currents through this device are in the range of 0.67 nA at an applied voltage of 2.6 V, corresponding to a current density of 1.4 $\mu A/cm^2$ at an electrical field of 250 kV/cm. For $GdScO_3$ with a film thickness of 112 nm, the leakage current density is only 0.85 $\mu A/cm^2$ at 250 kV/cm, whereas a 112 nm thick $LaScO_3$ film shows a slightly higher leakage of 6 $\mu A/cm^2$ at 250 kV/cm. Dielectric breakdown of $GdScO_3$ occurs at 1.2 MV/cm. For $DyScO_3$ breakdown is observed at 1 MV/cm and for $LaScO_3$ it takes place at over 600 kV/cm.

6 Summary and conclusion

PLD from sintered targets has resulted in good quality, epitaxial scandate films of $GdScO_3$, $LaScO_3$, and $DyScO_3$. In order to study the epitaxy, several different crystalline oxides have been used as substrates. All films show relatively high dielectric constants κ in comparison to other alternative gate dielectric candidates [2]. In addition, low leakage currents were observed. Optical measurements demonstrate a wide bandgap of the amorphous (> 5.5 eV) as well as of the epitaxial (> 5.8 eV) films. Scandate films could also be grown in an oxygen-free atmosphere with correct stoichiometry and comparable electrical properties. Such an oxygen-free deposition route suggests the possibility of growing scandate films onto silicon without a parasitic SiO_2 interlayer. Finally, the results illustrate the promise of rare earth scandates as the gate insulator for future silicon-based MOSFET devices. Presently, studies on thinner layers with an equivalent oxide thickness below 1 nm are in progress.

ACKNOWLEDGEMENTS This work was supported by the Deutsche Forschungsgemeinschaft (Graduiertenkolleg 549 Universität Köln, "Non-centrosymmetric Crystals"). J.L. F.and E. C. gratefully acknowledge the financial support of the National Science Foundation under Grant No. 0218288. W. T., Y. J., and D.G. S. acknowledge the support of the Semiconductor Research Corporation.

REFERENCES

1 The International Technology Roadmap for Semiconductors, ITRS 2003 Edition, USA (2003) http://public.itrs.net/
2 D.G. Schlom, J.H. Haeni, MRS Bulletin **27**, 198 (2002)
3 J. Schubert, O. Trithaveesak, A. Petraru, C.L. Jia, R. Uecker, P. Reiche, D.G. Schlom, Appl. Phys. Lett. **82**, 3460 (2003)
4 Landolt-Börnstein, *Numerical Data and Functional Relationships in Science and Technology* K.H. Hellwege, A.M. Hellwege (Eds.) (Springer, Berlin 1976), New Series, Group III, pp. 11–13
5 K.J. Hubbard, D.G. Schlom, J. Mater. Res. **11**, 2757 (1996)
6 C. Zhao, T. Witters, B. Brijs, H. Bender, O. Richard, M. Caymax, T. Heeg, J. Schubert, V.V. Afanas'ev, A. Stesmans, D.G. Schlom, Appl. Phys. Lett. **86**, 132 903 (2005)
7 V.V. Afanas'ev, A. Stesmans, C. Zhao, M. Caymax, T. Heeg, J. Schubert, Y. Jia, D.G. Schlom, G. Lucovsky, Appl. Phys. Lett. **85**, 5917 (2004)
8 J.C. Clark, J.P. Maria, K.J. Hubbard, D.G. Schlom, Rev. Sci. Instrum. **68**, 2538 (1997)
9 J. Lettieri, Y. Jia, S.J. Fulk, D.G. Schlom, M.E. Hawley, G.W. Brown, Thin Solid Films **379**, 64 (2000)
10 M. Siegert, W. Zander, J. Lisoni, J. Schubert, C. Buchal, Appl. Phys. A **69**, S779 (1999)
11 L. Beckers, J. Schubert, W. Zander, J. Ziesmann, A. Eckau, P. Leinenbach, C. Buchal, J. Appl. Phys. **83**, 3305 (1998)
12 X. Lu, Z. Liu, Y. Wang, Y. Yang, X. Wang, H. Zhou, B. Nguyen, J. Appl. Phys. **94**, 1229 (2003)
13 http://www.genplot.com/RUMP/index.htm
14 J.B. Nelson, D.P. Riley, Proc. Phys. Soc. London **57**, 160 (1945)
15 S.G. Lim, S. Kriventsov, T.N. Jackson, J.H. Haeni, D.G. Schlom, A.M. Balbashov, R. Uecker, P. Reiche, J.L. Freeouf, G. Lucovsky, J. Appl. Phys. **91**, 4500 (2002)
16 T. Heeg, M. Wagner, J. Schubert, C. Buchal, M. Boese, M. Luysberg, E. Cicerella, J.L. Freeouf, Microelectron. Eng. **80**, 150 (2005)
17 J.H. Haeni, Ph.D. Thesis, Pennsylvania State University, 2002. Available on-line at http://www.etda.libraries.psu.edu/theses/approved/WorldWideIndex/ETD-181/